The Microfabrication of Capacitive Ultrasonic Transducers

Xuecheng Jin, *Student Member, IEEE,* Igal Ladabaum, *Student Member, IEEE,* and Butrus T. Khuri-Yakub, *Fellow, IEEE*

***Abstract*— Surface-micromachined capacitive ultrasonic transducers, which are suitable for operation in both air and water, have been fabricated and tested. Amorphous silicon is used as a sacrificial layer because of its good etching selectivity versus a nitride membrane, and improved cell-size control is obtained by lithographic definition of cavity walls. In addition, appropriate feature designs based on two-dimensional (2-D) process simulations make it possible to achieve device cavity sealing with g-line optical lithography. Transmission experiments in both water and air are presented. A dynamic range in excess of 110 dB is observed in air at 2.3 MHz. In water, a single pair of transducers is able to operate from 2 to 15 MHz. When tuned, a 3.5-MHz tone burst results in a received signal with better than 60-dB signal-to-noise ratio (SNR). The transducer behavior agrees with a theoretical understanding of transducer dynamics. The dynamic ranges achieved in this paper are the best reported to date for surface-micromachined capacitive ultrasonic transducers. [274]**

***Index Terms*— Capacitive ultrasonic transducer, fabrication process, sacrificial etching, surface micromachining, vacuum sealing.**

I. Introduction

Ultrasound is used in a wide variety of applications which can be characterized as either sensing modalities or actuating modalities. Examples of sensing applications include medical imaging, nondestructive evaluation (NDE), ranging, and gas-flow metering. As an actuating mechanism, ultrasound is used in industrial cleaning, soldering, and medical therapy. For years, piezoelectric ceramics and engineering cleverness have enabled a significant number of ultrasonic devices and systems [9], but fruitful applications are restricted by the piezoelectrics' limitations. Piezoelectric transducers require strict geometric tolerances, which, in turn, limit possible array configurations and electrical characteristics. Furthermore, piezoelectrics depole at relatively low temperatures. As an alternative, capacitive ultrasonic transducers are some of the promising candidates.

Micromachined ultrasonic transducers (MUT's) provide advantages in size reduction and potential electronic integration. The successful microfabrication of capacitive acoustic transducers consisting of a suspended membrane over a backplate was reported within the last decade [8]. Capacitive ultrasonic transducers have been reported in [1], [17], [19], [20], and [22], and, recently, capacitive-micromachined ultrasonic transducers (cMUT's) were reported in [5]–[7]. Further improvements in [10], [12], [13], and [21] extend the performance and understanding of cMUT's. In addition, concurrent development efforts are reported with contoured backplate devices in [2] and with BiCMOS electronics integration in [4]. Piezoelectric-micromachined ultrasonic transducers (pMUT's) are found in [3], [18], and [23].

In contrast to previous publications, this paper focuses on the realization of designs based on the reported theoretical understanding and, more specifically, the microfabrication process. In order to achieve better sensitivity and dynamic range, improvement has been made over previous work [12], [13], where the device suffers from cell-sizing variation due to timed oxide etching and from nitride membrane thickness variation due to its relatively low selectivity against the sacrificial thermal oxide layer. In this work, amorphous silicon is used as a sacrificial layer rather than thermal oxide to give better etching selectivity against the nitride membrane, and better cell-size control is obtained by lithographic definition of cavity walls instead of timed etching. In addition, appropriate feature sizing based on computer simulation makes it possible to achieve device cavity sealing with low-cost g-line optical lithography instead of the submicron electron beam lithography [21]. Furthermore, the fully surface-micromachined fabrication process presented here provides an option to integrate electronics into cMUT's.

In this paper, a brief introduction to transducer electrical equivalent circuit model is presented in Section II followed by a discussion of the fabrication process in Section III. In Section IV, experimental results are described. Section V concludes the paper.

II. Transducer Electrical Equivalent Circuit Model

A cMUT consists of metalized membranes (top electrode) suspended above heavily doped silicon bulk (bottom electrode). A schematic of one element of the device is shown in Fig. 1, where d is the diameter of the active membrane, t_n is the membrane thickness, t_a is the air-gap thickness, t_b is the insulating layer thickness, and sp is the side-wall spacing dimension. A transducer consists of many such elements. When a dc voltage V_{dc} is applied between the two electrodes, Coulomb forces attract them together. At the same time, the residual stress within the membrane resists the attraction. If the membrane is driven by an ac voltage V_{ac}, significant ultrasound generation results. Conversely, significant detection currents are generated when the membrane is biased

Manuscript received July 8, 1997; revised March 20, 1998. This work was supported by grants from the United States Office of Naval Research and a Fellowship from the National University of Singapore, Singapore. Subject Editor, S. D. Senturia.

The authors are with the E. L. Ginzton Laboratory, Stanford University, Stanford, CA 94305 USA (e-mail: xcjin@alumni.stanford.org).

Publisher Item Identifier S 1057-7157(98)06346-X.

1057–7157/98$10.00 © 1998 IEEE

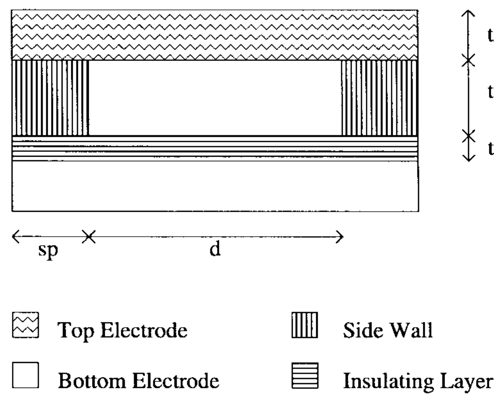

Fig. 1. Schematic of one element of a cMUT.

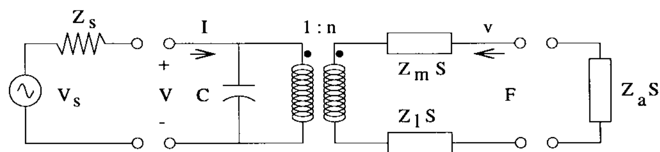

Fig. 2. Equivalent circuit of cMUT.

appropriately and subjected to ultrasonic waves. For a desired electrical field applied across the top and bottom electrodes, a higher dc bias voltage with thicker layers or a lower dc bias voltage with thinner layers are needed. The former provides easier control of the vertical dimension in micromachining and higher membrane displacement. The latter provides better step coverage in layer deposition and low-voltage operation.

The recently developed transducer electrical equivalent circuit model [20] as shown in Fig. 2 makes it possible to analyze the tradeoffs and optimize the cMUT's structure. In this model, mechanical parameters, average membrane velocity v, and force applied to the membrane F are transformed into electrical parameters current I and voltage V by a transformer ratio n, which is a function of the dc bias voltage $V_{\rm dc}$ and various thickness and dielectric properties of the layered materials. In the mechanical port, three impedances are important, and all are a function of device area S. Z_m is the membrane mechanical impedance, Z_a is the acoustic load impedance, and Z_l is the lumped term accounting for all the losses in the transducer. In the electrical port, there is a parasitic capacitance C due to the capacitive nature of cMUT and the input impedance of the receiver electronics Z_s or the source impedance Z_s of the transmitter signal V_s.

The model indicates that the variation of cell size and membrane thickness will affect the transducer performance [20]. As shown in Figs. 3 and 4, the transducer resonant frequency with air-loading shifts about 3.5% from 2.29-MHz nominal value when either the cell radius changes 2% from its nominal value of 50 μm or the membrane thickness varies 5% from its nominal value of 1 μm. So, it is critically important to have a robust fabrication process, especially for airborne transducers which operate in resonant mode and are made from a plurality of membranes. For immersion transducers, the above issue is relatively less important since the water loading rather than the membrane's mechanical impedance dominates the total impedance, and the transducers usually do not operate in resonant mode.

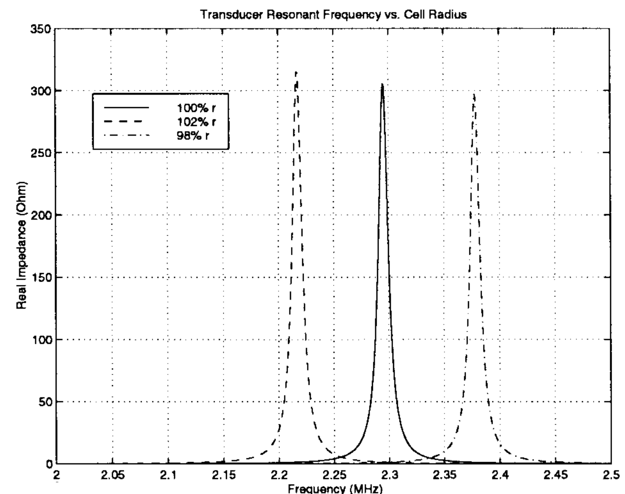

Fig. 3. Transducer resonant frequency change with cell size.

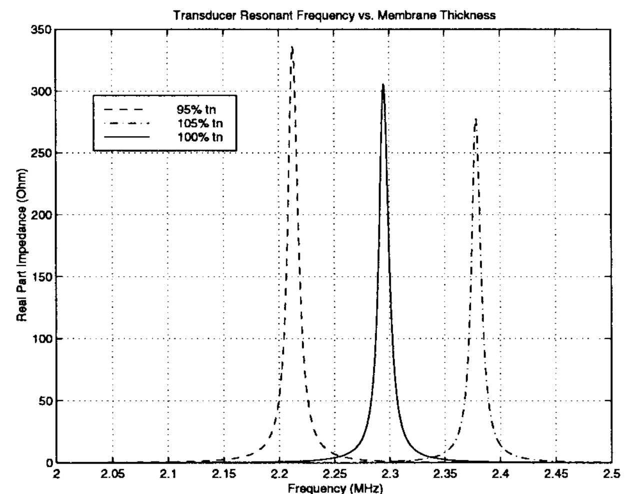

Fig. 4. Transducer resonant frequency change with membrane thickness.

III. Fabrication

The fabrication scheme of the cMUT's used to generate the results herein reported is found in Fig. 5. It is fully surface micromachined and compatible with standard CMOS fabrication processes. A 4-in n-type (100) silicon wafer is heavily doped with 4-h phosphorus gas phase drive in at 1000°C to achieve good conductivity at the wafer surface. Better than 1.5-Ω/□ resistivity can be routinely achieved. A thin layer of low-pressure chemical-vapor deposition (LPCVD) nitride is then deposited at 800°C as an etch stop in the potassium hydroxide and water (KOH) sacrificial etching to be performed later. Amorphous silicon is subsequently deposited at 560°C to form the sacrificial layer. Deposited amorphous silicon is dry-etch patterned into hexagonally shaped islands to define the active transducer regions.

A second layer of nitride is then deposited by LPCVD at 800°C to form a thin membrane. The silane and ammonia ratio is controlled such that a residual stress of 60 MPa is obtained.

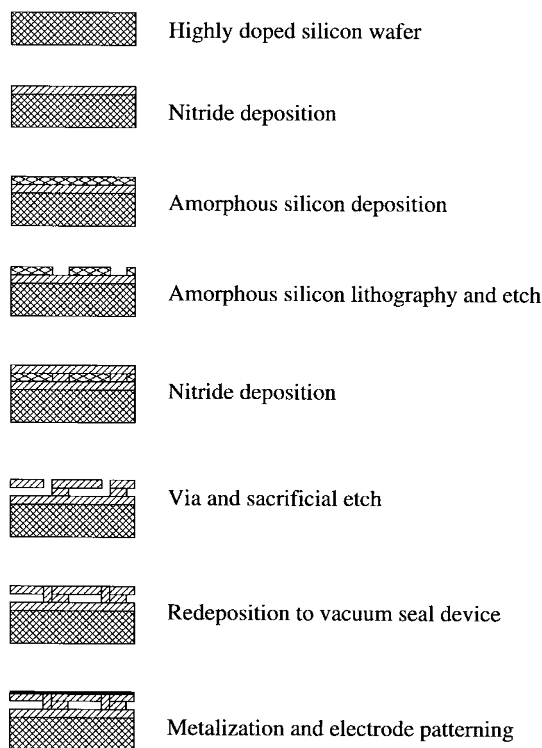

Fig. 5. Major steps of cMUT fabrication.

Both the residual stress and membrane thickness affect the resonant frequency and the voltage at which an electrostatic pull-in phenomenon is observed. Vias are dry etched to allow sacrificial etching in KOH at 75°C followed by vacuum sealing with nitride or low-temperature oxide (LTO) deposition. The dimension of the via has implications on the mechanism with which the sealing is performed.

Finally, aluminum is sputtered and wet-etch patterned to act as the top electrode. The same aluminum deposition also defines bonding contacts to the bottom electrode through a lithographically defined trench in silicon bulk. A scanning electron microscope (SEM) image of the top view of the transducer is shown in Fig. 6.

IV. Discussion

As discussed in the previous section, the transducer geometry controls its performance characteristics. Both process capability and device performance requirements put boundary conditions on the device dimensions. In this paper, special attention has been paid to the following feature sizes.

A. Cell Dimension

In order for consistent transducer performance over a wide frequency range, cell size is desired to change proportionally with the wavelength at which ultrasound operates. For example, at operating frequencies of 1–2 MHz in air and 5–10 MHz in water, the maximum cell dimension ranges from 20 to 100 μm. Since transducer impedance and resonant frequency is a very strong function of the device cell size [14], timed etching does not provide enough tolerance for high-performance cMUT's. Instead, lithographic definition can

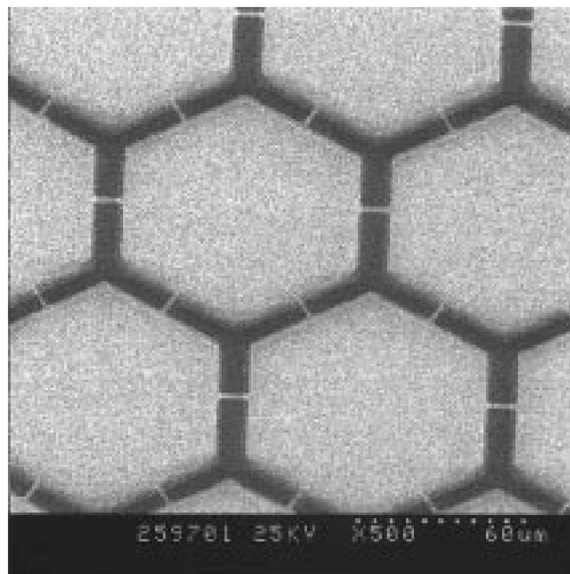

Fig. 6. SEM top view of the cMUT.

guarantee that transducers are reproducible. In the experiment, only the fluctuation of the third most significant digit of resonant frequency is observed. This greatly reduces the minimum bandwidth requirement of the cMUT's to be paired as transmitters and receivers in narrow-band applications.

Furthermore, when the lateral cell size is controllable, it can be used to make up for process limitations of vertical dimension and realize the desired performance characteristics for the cMUT's. Utilizing lithographic definition in transducer cell sizing rather than timed etching is one of the significant improvements in the paper.

B. Via Dimension

The dimension of the vias should be big enough for sacrificial etching and small enough for sealing, which is necessary for immersion operation. When submicron electron beam lithography is available for via definition, a thin layer of nitride deposition seals the cavity successfully at several hundred militorr vacuum [13]. The results are confirmed with computer simulations in SPEEDIE [21] [a two-dimensional (2-D) process simulator developed at Stanford University] as shown in Fig. 7 for LTO deposition and Fig. 8 for nitride deposition. Here, the sticking coefficient of depositing species does not matter since the access hole is only 0.25 μm in diameter.

In order to reduce the process cost, g-line optical lithography is preferred. In addition, larger vias will increase the speed of sacrificial etching. SPEEDIE simulation indicates it is possible to seal a cavity with several micron wide vias by depositing low-sticking coefficient species. LTO is one of the candidates which has a sticking coefficient more than two orders of magnitude higher than nitride [22]. Fig. 9 is a SPEEDIE simulation result verifying a sealed cavity with a 2-μm via by LTO deposition at 400°C. If the same via is sealed with nitride, the entire cavity tends to be filled due to its much lower sticking coefficient as shown in Fig. 10. This will greatly degrade the dimension control discussed above. An SEM of

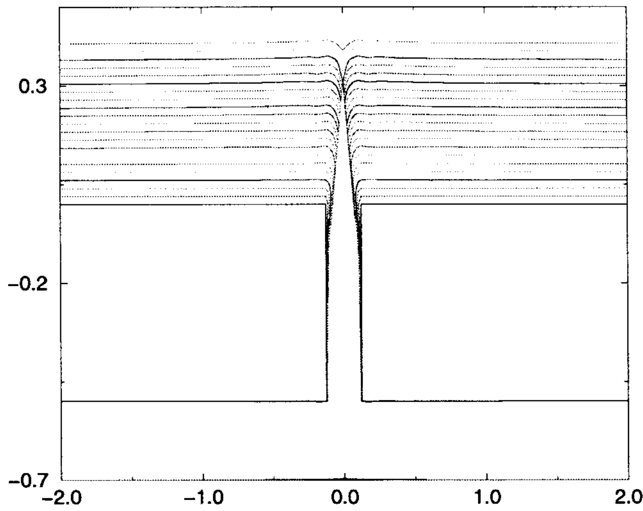

Fig. 7. SPEEDIE simulation for LTO sealing of 0.25-μm via.

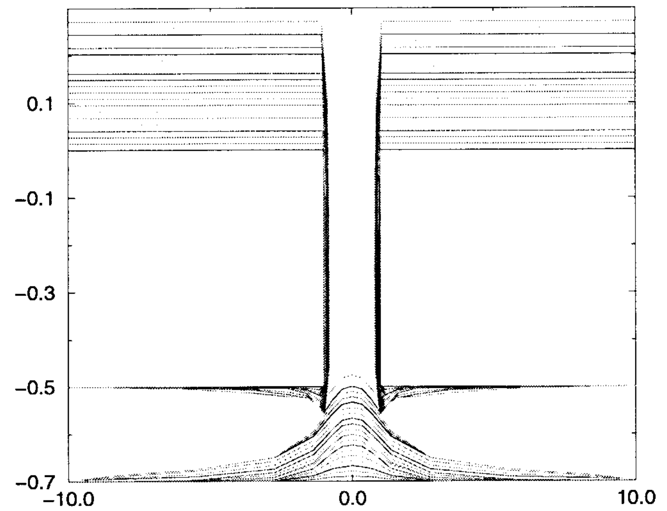

Fig. 9. SPEEDIE simulation for LTO sealing of 2-μm via.

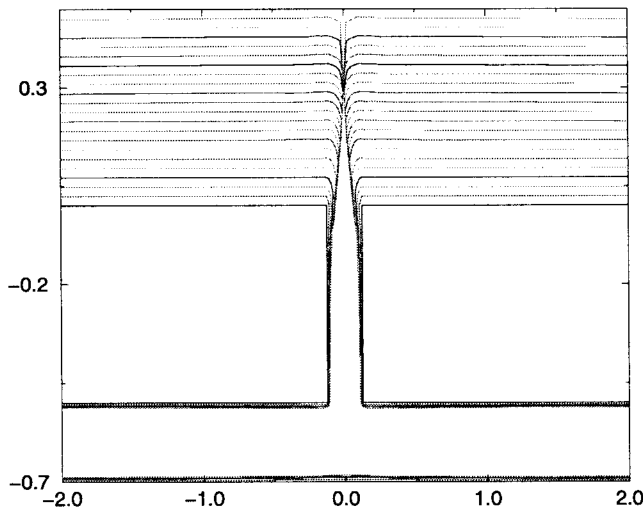

Fig. 8. SPEEDIE simulation for nitride sealing of 0.25-μm via.

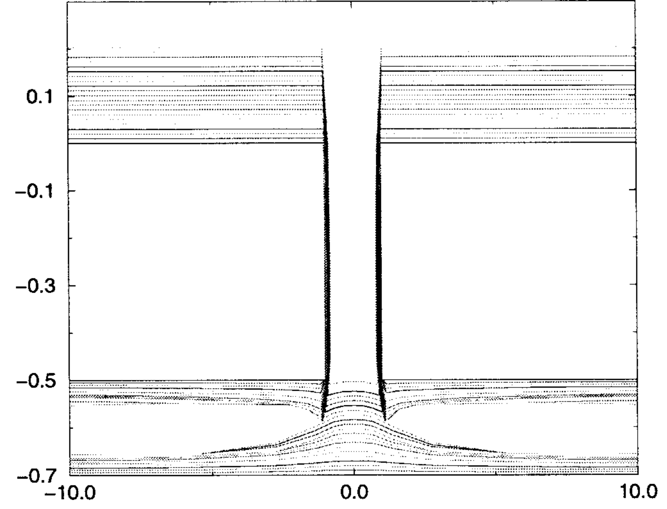

Fig. 10. SPEEDIE simulation for nitride sealing of 2-μm via.

LTO sealing of a 2-μm via is found in Fig. 11. It is observed that the LTO filling is limited to only a few microns.

C. Protection Nitride Thickness

The bottom protection nitride is required by the process to act as a KOH etch stop, but it is undesired for optimal transducer performance since it reduces the effective electric field applied across the device, especially in an immersion transducer which has a relatively smaller air gap. So, this nitride layer should be thick enough to sustain the variation in the following dry etching steps and thin enough not to cause much decrease in the electric field applied to the device. As a start, a very conservative value of 3000–5000 Å is used depending on the air gap and membrane thickness.

D. Sacrificial Layer Thickness

The amorphous silicon acts as a sacrificial layer in the process. Compared to thermal oxide used in previous work [10], [12], [14], amorphous silicon is preferred due to its two orders of magnitude higher etching selectivity against nitride [23]. In terms of transducer efficiency, a thinner air gap is favorable, but this will pose a problem during membrane release as well as by limiting the maximum membrane displacement. The thickness ranges from 2000 Å to 1 μm depending on whether the transducer will be used in gases, or liquids, as a receiver or transmitter.

Using amorphous silicon as a sacrificial layer for the nitride membrane is another significant improvement in the paper to give precise control of transducer resonant frequency and impedance level. In addition, it allows larger membranes for air applications where the resonant frequency of the membrane can be reduced to hundreds of kilohertz.

E. Suspended Membrane Thickness

The suspended nitride membrane is metalized to form the upper electrode. A low-stress nitride with 60-MPa tensile stress [23] is used. Similar to the case of the sacrificial layer, the

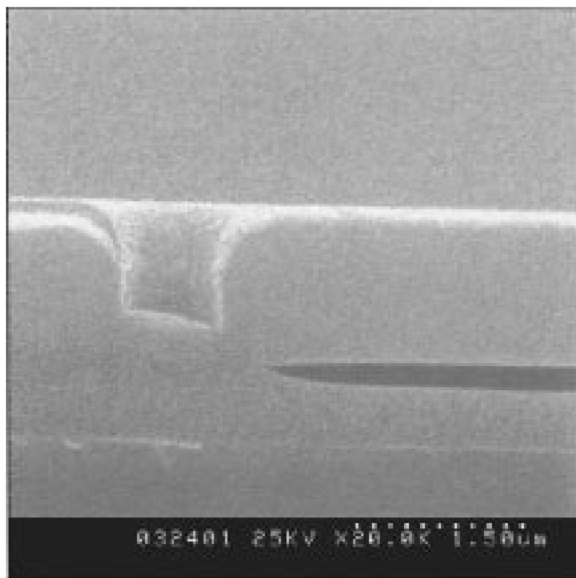

Fig. 11. SEM of LTO sealing of 2-μm via.

membrane should be as thin as possible for most efficient operation, but it should be thick enough to avoid electrostatic pull in and provide enough stress for successful releasing after sacrificial etching. A typical value is 0.5–2 μm including the redeposition for vacuum sealing.

F. Metal Thickness

Aluminum is used for the top electrode. A thick layer is preferred to reduce the serial resistance of the transducer, but it should not be so thick that its weight poses significant loading to the transducer membrane (i.e., changing the mechanical impedance of the membrane). A typical value is 2000 Å. Aluminum sputtering is performed rather than evaporation for better step coverage over varying topology on cMUT's surface.

V. Experiments

The experiments in this paper are performed with the help of a custom electronic setup. Time domain data are captured with an 8-b digitized oscilloscope, and frequency domain data are captured with a network analyzer. Subsequently, the data are transferred to a computer for display. In certain circumstances, data sample averaging is performed to obtain better signal-to-noise ratio (SNR). The ac excitation signal is provided by a pulse function generator with 50-Ω output resistance. A transconductance amplifier conditions the received signal.

There are two types of cMUT's used in the experiments as described in Table I. Type I is designed for air operation where the transducer is not sealed and larger in cell size. Type II is designed for immersion operation with smaller and sealed cavities. For each type of cMUT, the size and dc bias of the device can be varied for either impedance or power purpose.

A. Air Transducer

Fig. 12 shows the impedance of an air cMUT Type I with 1-cm^2 size and biased at 30-V dc voltage. The simulation results based on the electrical equivalent circuit model are shown in solid line, and the actual measurements are shown in dashed lines. The negative imaginary parts indicate capacitive parasitics. Both the theoretical prediction and actual device give a resonant frequency around 2.3 MHz. In addition, the device has comparable real and imaginary impedance at resonance. This makes it possible to tune out the negative imaginary part with a serial inductor without severely degrading bandwidth. As shown in Fig. 13, this device is able to detect the ultrasound transmitted in air with better than 30-dB SNR after 16 sample averages. This result is obtained when a 20-cycle 1-mV ac tone burst at a 2.3-MHz resonant frequency

TABLE I
PARAMETERS OF cMUT'S FOR AIR AND IMMERSION EXPERIMENT

Type	Operation	d	sp	t_a	t_n	t_b	Cavity
I	Air	100um	10um	1.0um	0.5um	0.4um	Unsealed
II	Immersion	30um	6.5um	0.3um	1.3um	0.6um	Sealed

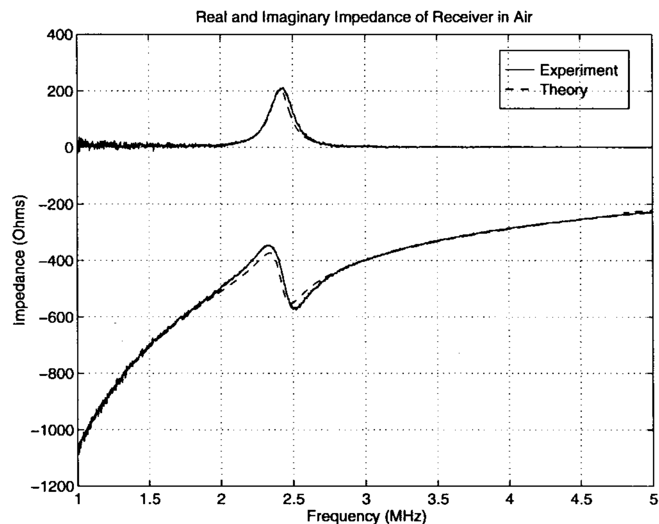

Fig. 12. Transducer impedance with air loading.

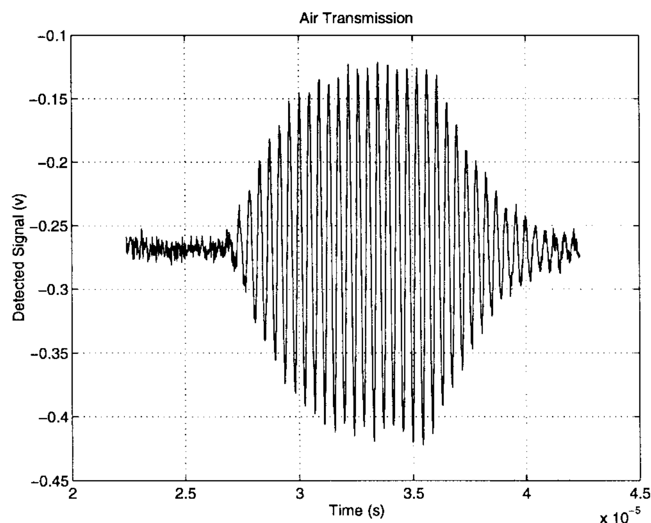

Fig. 13. Twenty-cycle burst transmission in air at 2.3 MHz.

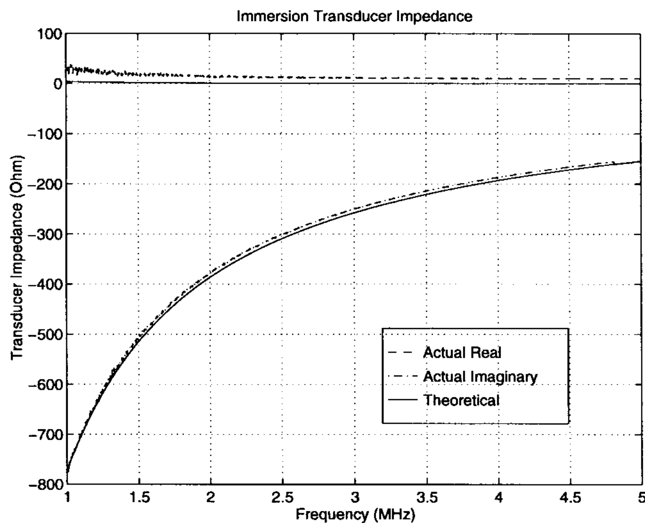

Fig. 14. Transducer impedance with water loading.

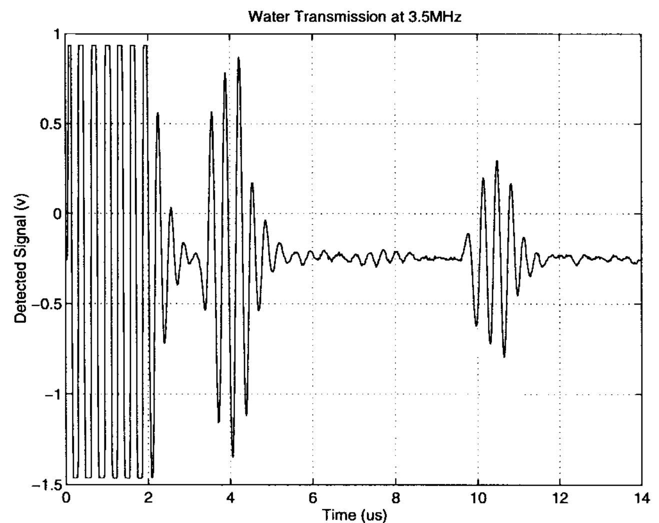

Fig. 15. Three-cycle burst transmission in water at 3.5 MHz.

is applied to the transmitter which has identical parameters to the receiver. When ac excitation is increased to 10 V, a dynamic range in excess of 110 dB is observed in air operation after 64 sample averages. It is noticed that a nonzero loss term is included in the model to obtain the theoretical results shown in Fig. 12, indicating potential possibility for further improvement of transducer dynamic range.

B. Immersion Transducer

In fact, the same device can be used for both air and water transmission since the fabrication process is designed to yield vacuum-sealed cavities, but a good air transducer is not necessarily the best immersion transducer due to the different loading effects of air and water.

Fig. 14 shows the impedance of an immersion cMUT Type II with 0.25-cm^2 size and biased at 30-V dc voltage. The simulation results based on the electrical equivalent circuit model are shown in solid line, and the actual measurements are shown in dashed lines. It is noticed that the real part of the immersion transducer impedance is significantly lower than that of the air-loaded transducer in both simulation and actual measurement. In future designs of immersion transducers, the geometry of the device (gap thickness, membrane thickness, and radius) and bias voltage of the device can be modified to optimize the transducers for water operation, or more specifically, to increase the absolute value of the real part of the transducer impedance to the level comparable to the electronics.

When the device is used as a receiver and tuned with a serial inductor, better than 60-dB SNR is observed in water transmission at 3.5 MHz, as shown in Fig. 15. In the figure, electromagnetic feedthrough is followed by the acoustic signal indicating a 5-mm physical separation. In this experiment, the transmitter is 1 cm^2 to increase the acoustic power. The lower dynamic range compared to air operation is mainly due to the higher imaginary-to-real impedance ratio. This leads to an impedance mismatch with transmitting and receiving electronics since the same electronic system is used for both air and water operation.

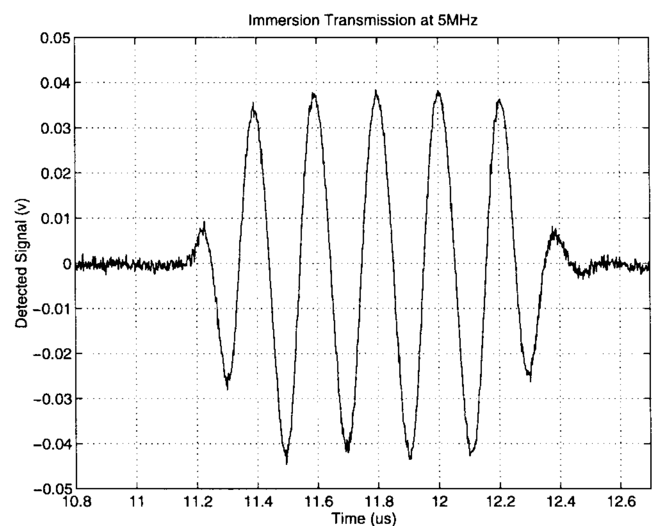

Fig. 16. Immersion transmission at 5 MHz.

Wide-band transmission is possible if the cMUT's operate less efficiently, which is true for untuned and unoptimized immersion transducers. Acoustic behavior is observed at 2–15 MHz as shown in Figs. 16–18, where five-cycle bursts are transmitted at 5, 10, and 15 MHz, respectively. In this experiment, both the receiver and transmitter are 1 cm^2.

The dynamic ranges of both air and immersion cMUT's achieved in this paper are compared with previous results and the idealized theoretical limits[1] as shown in Table II. The air transducer exhibits a 30-dB improvement and the immersion transducer 12-dB improvement, and both have substantial potential for further improvement.

VI. Conclusion

This paper presents a fully surface-micromachined fabrication scheme which enables the realization of designs

[1] The theoretical limit of the dynamic range of cMUT's is calculated from the ratio of the maximum membrane displacement (pull-in limit) to the equivalent membrane displacement of the thermal noise of the transducer.

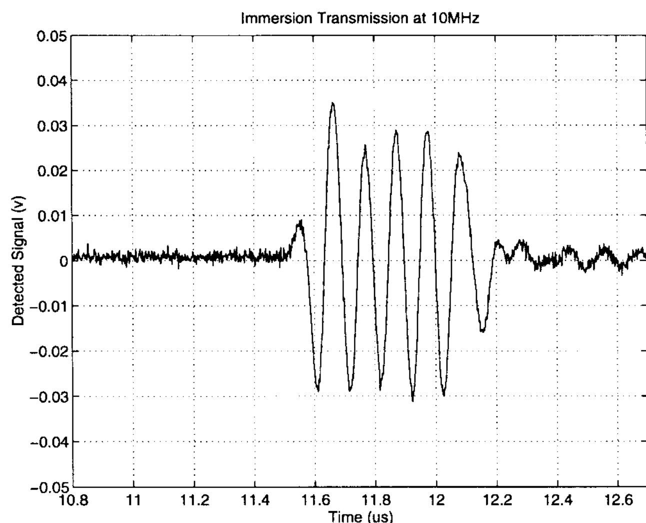

Fig. 17. Immersion transmission at 10 MHz.

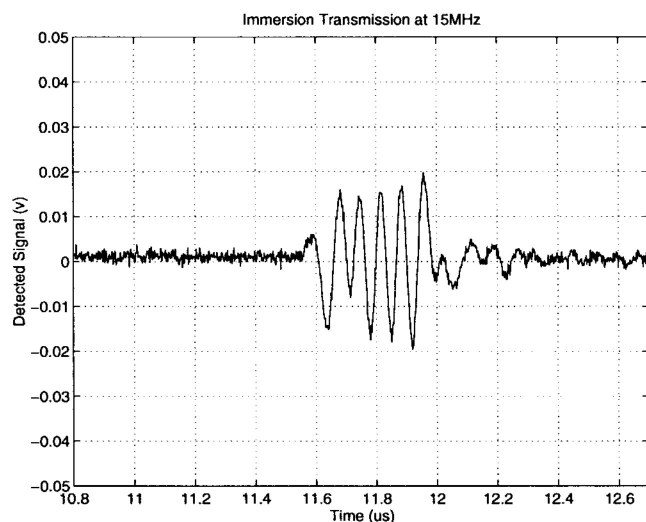

Fig. 18. Immersion transmission at 15 MHz.

TABLE II
COMPARISON OF cMUT'S DYNAMIC RANGE

Item	This work	Previous work	Theoretical limit
Air cMUTs	110 dB	80dB [11]	130dB [13]
Immersion cMUTs	60dB	48dB [13]	130dB [13]

based on a theoretical understanding of transducer dynamics. Amorphous silicon is used as a sacrificial layer to form sealed nitride cavities. It is important to appreciate the etching selectivity of silicon versus nitride in KOH, which allows the realization of the design. A dynamic range in excess of 110 dB is achieved in air at 2.3 MHz. In water operation, a single pair of cMUT's can transmit 2–15-MHz ultrasound. When tuned, a 3.5-MHz tone burst results in better than 60-dB SNR. The dynamic ranges achieved in this paper are the best reported to date for surface-micromachined capacitive ultrasonic transducers. It is anticipated that future optimized designs will result in better immersion operation.

The experiments show cMUT's are a feasible alternative to piezoelectric transducers in many applications. Furthermore, cMUT's can operate at high temperature (they do not have a Curie temperature), arrays can be fabricated at lower cost, and the electrical impedance of a cMUT element can be designed to optimize the noise performance of receiver electronics.

ACKNOWLEDGMENT

Special thanks are due to Dr. J. P. McVittie, T. Carver, P. Prather, and other technical staff at Ginzton Laboratory and the Center for Integrated Systems of Stanford University.

REFERENCES

[1] M. J. Anderson, J. A. Hill, C. M. Fortunko, N. S. Dogan, and R. D. Moore, "Broadband electrostatic transducers: Modeling and experiments," *J. Acoust. Soc. Amer.*, vol. 97, no. 1, pp. 262–272, Jan. 1995.

[2] A. G. Bashford and D. A. Hutchins, "Characteristics of ultrasonic micromachined capacitance transducers in water," in *Ultrasonics Symp., IEEE Ultrasonics, Ferroelectrics, and Frequency Control Society,* San Antonio, TX, 1996, pp. 955–958.

[3] J. J. Bernstein, S. L. Finberg, K. Houston, L. C. Niles, H. D. Chen, E. L. Cross, K. K. Li, and K. Udayakumar, "Micromachined high frequency ferroelectric sonar transducers," *IEEE Trans. Ultrason., Ferroelect., Freq. Contr.,* vol. 44, no. 5, pp. 960–969, 1997.

[4] P. Eccardt, K. Niederer, T. Scheiter, and C. Hierold, "Surface micromachined ultrasound transducers in CMOS technology," in *Ultrasonics Symp., IEEE Ultrasonics, Ferroelectrics, and Frequency Control Society,* San Antonio, TX, Nov. 1996, pp. 959–962.

[5] M. I. Haller, "Micromachined ultrasonic devices and materials," Ph.D. dissertation, Stanford Univ., Stanford, CA, 1997.

[6] M. I. Haller and B. T. Khuri-Yakub, "A surface micromachined electrostatic ultrasonic air transducer," *IEEE Trans. Ultrason., Ferroelect., Freq. Contr.,* vol. 43, no. 1, pp. 1–6, 1996.

[7] ——, A surface micromachined electrostatic ultrasonic air transducer, in *Ultrasonics Symp., IEEE Ultrasonics, Ferroelectrics, and Frequency Control Society,* Cannes, France, 1994, pp. 1241–1244.

[8] D. Hohm and G. Hess, "A subminiature condenser microphone with silicon-nitride membrane and silicon backplate," *J. Acoust. Soc. Amer.,* vol. 85, no. 1, pp. 476–480, Jan. 1989.

[9] G. S. Kino, *Acoustic Waves: Devices, Imaging, and Analog Signal Processing.* Englewood Cliffs, NJ: Prentice-Hall, 1987.

[10] I. Ladabaum, X. C. Jin, and B. T. Khuri-Yakub, "Air coupled through transmission of aluminum and other recent results using MUT's," in *Ultrasonics Symp., IEEE Ultrasonics, Ferroelectrics, and Frequency Control Society,* Toronto, Canada, Oct. 1997, pp. 983–986.

[11] I. Ladabaum, X. C. Jin, H. T. Soh, F. Pierre, A. Atalar, and B. T. Khuri-Yakub, "Micromachined ultrasonic transducers: Toward robust models and immersion devices," in *Ultrasonics Symp., IEEE Ultrasonics, Ferroelectrics, and Frequency Control Society,* San Antonio, TX, Nov. 1996, pp. 335–338.

[12] I. Ladabaum, B. T. Khuri-Yakub, and D. Spoliansky, "Micromachined ultrasonic transducers: 11.4 MHz transmission in air and more," *Appl. Phys. Lett.,* vol. 68, no. 1, pp. 7–9, Jan. 1996.

[13] I. Ladabaum, B. T. Khuri-Yakub, D. Spoliansky, and M. I. Haller, "Micromachined ultrasonic transducers MUT's," in *Ultrasonics Symp., IEEE Ultrasonics, Ferroelectrics, and Frequency Control Society,* Seattle, WA, Nov. 1995, pp. 501–504.

[14] J. P. McVittie, "Standard etch rate data sheet," *Stanford University Nanofacility Reference Manual,* Stanford Univ., Stanford, CA, 1996.

[15] ——, "Private communication," Center for Integrated Systems, Stanford Univ., Stanford, CA, 1997.

[16] J. P. McVittie, D. S. Bang, J. S. Han, K. Hsiau, J. Li, and J. Zheng, "Stanford profile emulator for etching and deposition in IC engineering," *SPEEDIE 3.0 Manual,* Stanford Univ., Stanford, CA, 1995.

[17] M. Pentti, F. Tsuzuki, H. Vaataja, and K. Sasaki, "Electroacoustic model for electrostatic ultrasonic transducers with v-grooved backplates," *IEEE Trans. Ultrason., Ferroelect., Freq. Contr.,* vol. 42, no. 1, pp. 1–7, 1995.

[18] G. Percin and B. T. Khuri-Yakub, "Micromachined 2-D array piezoelectrically actuated flextensional transducer," in *Ultrasonics Symp., IEEE Ultrasonics, Ferroelectrics, and Frequency Control Society,* Toronto, Canada, Oct. 1997, pp. 959–962.

[19] M. Rafiq and C. Wykes, “The performance of capacitive ultrasonic transducers using v-grooved backplates,” *Meas. Sci. Technol.,* vol. 2, no. 2, pp. 168–174, Feb. 1991.
[20] D. W. Schindel, D. A. Hutchins, L. Zou, and M. Sayer, “The design and characterization of micromachined air-coupled capacitance transducers,” *IEEE Trans. Ultrason., Ferroelect., Freq. Contr.,* vol. 42, no. 1, pp. 42–50, 1995.
[21] H. T. Soh, I. Ladabaum, A. Atalar, C. F. Quate, and B. T. Khuri-Yakub, “Silicon micromachined ultrasonic immersion transducers,” *Appl. Phys. Lett.,* vol. 69, no. 24, pp. 3674–3676, 1996.
[22] K. Suzuki, K. Higuchi, and H. Tanigawa, “A silicon electrostatic ultrasonic transducer,” *IEEE Trans. Ultrason., Ferroelect., Freq. Contr.,* vol. 36, pp. 620–627, Nov. 1989.
[23] R. M. White, R. J. Wicher, S. W. Wenzel, and E. T. Zellers, “Plate mode ultrasonic oscillator sensors,” *IEEE Trans. Ultrason., Ferroelect., Freq. Contr.,* vol. 34, no. 2, pp. 162–171, 1987.

Xuecheng Jin (S’93) received the B.Eng. degree in biomedical engineering from Tsinghua University, China, in 1990 and the M.Eng. degree in computer engineering from the National University of Singapore, Singapore, in 1994. He is currently working towards the Ph.D. degree in electrical engineering at Stanford University, Stanford, CA.

He was with Oriental Star Microcomputers, China, until 1992, where he designed analog and digital circuits for various instrumentation. He then was with Texas Instruments Pte Ltd., Singapore, where he designed computer vision algorithms and software codes for real-time postmount die inspection in die bonder machines. In 1995, he joined the faculty of the Electrical Engineering Department, National University of Singapore, as a Senior Tutor, where he was primarily engaged in research into solid-state sensors and actuators, MEMS and micromachining technology, CMOS integrated circuit design, bioinstrumentation and its miniaturization, medical image processing, and computer vision.

Mr. Jin serves as a Reviewer for several international journals with about 20 publications. He received the RWB Stephens Best Student Paper Prize at the Ultrasonics International Conference, Delft, The Netherlands, in July 1997 and the Whitaker Student Paper Finalist Certificate at the IEEE International Conference on Engineering in Medicine and Biology, Baltimore, MD, in November 1994.

Igal Ladabaum (S’91) received the B.S. degree in bioengineering from the University of California, Berkeley, in 1992 and the M.S. degree in electrical engineering from Stanford University, Stanford, CA, in 1996. He is currently working towards the Ph.D. degree at Stanford University.

He was a Jean Monnet Scholar from 1992 to 1993 at the Ecole Polytechniquethen, Paris, France. He was also a Staff Engineer at Air Liquide. He is interested in the techniques of micromachining and their application to the realization of novel transducers. Most of his effort is directed toward the development and application of ultrasonic transducers. He has contributed several journal and conference papers and is pursuing patents for some of his work on ultrasonic transducers.

Mr. Ladabaum is a Member of the Acoustical Society of America. He has received numerous awards, including the Best Student Paper Prize at the International Conference of Micro and Nano-Engineering, Aix en Provence, France, in 1995 and the RWB Stephens Best Student Paper Prize in Ultrasonics International Conference, Delft, The Netherlands, in July 1997.

Butrus T. Khuri-Yakub (S’70–M’76–SM’87–F’95) was born in Beirut, Lebanon. He received the B.S. degree in 1970 from the American University of Beirut, Beirut, the M.S. degree in 1972 from Dartmouth College, Hanover, NH, and the Ph.D. degree in 1975 from Stanford University, Stanford, CA, all in electrical engineering.

He joined the research staff at the E. L. Ginzton Laboratory, Stanford University, in 1976 as a Research Associate. He was promoted to Senior Research Associate in 1978 and to Professor of Electrical Engineering (Research) in 1982. He has served on many university committees such as graduate admissions, undergraduate academic council of the school of engineering, and others. He has taught both at the graduate and undergraduate levels for over 15 years, and his current research interests include *in situ* acoustic sensors (temperature, film thickness, resist cure, etc.) for monitoring and control of integrated circuits manufacturing processes; micromachining silicon to make acoustic materials; devices such as airborne and water immersion ultrasonic transducers and arrays and fluid ejectors; and the fields of ultrasonic nondestructive evaluation, acoustic imaging, and microscopy. He has authored about 300 publications and has been a principal inventor or coinventor of over 30 patents.

Dr. Khuri-Yakub is a Senior Member of the Acoustical Society of America and a Member of Tau Beta Pi. He was a Member of the AdCom of the IEEE Group on Ultrasonics Ferroelectrics and Frequency Control from 1994 to 1997. He is an Associate Editor of *Research in Nondestructive Evaluation*, a journal of the American Society for Nondestructive Testing. He received the Stanford University School of Engineering Distinguished Advisor Award in 1987 and the Medal of the City of Bordeaux for contributions to NDE in 1983.